



Published in final edited form as:

Oncogene. 2019 May ; 38(18): 3340–3354. doi:10.1038/s41388-018-0646-9.

ATDC Mediates a TP63-Regulated Basal Cancer Invasive Program

Phillip L. Palmbo^{1,7,*}, Yin Wang^{1,7}, Armand Bankhead^{2,3,7}, Alan J. Kelleher¹, Lidong Wang^{8,10}, Huibin Yang⁴, McKenzie L. Ahmet¹, Erica R. Gumkowski¹, Samuel D. Welling⁷, Brian Magnuson^{2,7}, Jacob Leflein⁷, Guadalupe Lorenzatti Hiles^{6,7}, Ethan Abel⁷, Michele L. Dziubinski^{5,7}, Sumithra Urs⁷, Mark Day⁶, Mats E. Ljungman^{4,7}, and Diane M. Simeone^{8,9,10}

¹Department of Internal Medicine, University of Michigan Medical Center, Ann Arbor, MI. 48109. USA.

²Department of Biostatistics, University of Michigan Medical Center, Ann Arbor, MI. 48109. USA.

³Department of Computational Medicine and Bioinformatics, University of Michigan Medical Center, Ann Arbor, MI. 48109. USA.

⁴Department of Radiation Oncology, University of Michigan Medical Center, Ann Arbor, MI. 48109. USA.

⁵Department of Molecular and Integrative Physiology, University of Michigan Medical Center, Ann Arbor, MI. 48109. USA.

⁶Department of Urology, University of Michigan Medical Center, Ann Arbor, MI. 48109. USA.

⁷Department of Translational Oncology Program, University of Michigan Medical Center, Ann Arbor, MI. 48109. USA.

⁸Department of Surgery, NYU Langone Health, New York, NY 10016.

⁹Department of Pathology, NYU Langone Health, New York, NY 10016.

¹⁰Department of Perlmutter Cancer Center, NYU Langone Health, New York, NY 10016.

Abstract

Basal subtype cancers are deadly malignancies but the molecular events driving tumor lethality are not completely understood. Ataxia-Telangiectasia Group D Complementing gene (ATDC, also known as TRIM29), is highly expressed and drives tumor formation and invasion in human bladder cancers but the factor(s) regulating its expression in bladder cancer are unknown. Molecular subtyping of bladder cancer has identified an aggressive basal subtype which shares molecular features of basal/squamous tumors arising in other organs and is defined by activation

Users may view, print, copy, and download text and data-mine the content in such documents, for the purposes of academic research, subject always to the full Conditions of use:http://www.nature.com/authors/editorial_policies/license.html#terms

*Corresponding Author. Address Correspondence and material requests to: Phillip L. Palmbo, M.D., Ph.D., Dept. of Internal Medicine, Hematology/Oncology Division, NCRC Building 520, Room 1345, 1600 Huron Parkway, Ann Arbor, MI 48109, ppalmbo@med.umich.edu, Phone: (734) 936-3591, Fax: (734) 647-6977.

Conflict of Interest: Authors have no financial conflicts to disclose.

Supplemental Material: Contains Supplemental Figures 1–7, Supplemental Material and Methods and Video.

of a TP63-driven gene program. Here we demonstrate that ATDC is linked with expression of TP63 and highly expressed in basal bladder cancers. We find that TP63 binds to transcriptional regulatory regions of ATDC and KRT14 directly, increasing their expression, and that ATDC and KRT14 execute a TP63-driven invasive program. *In vivo*, ATDC is required for TP63-induced bladder tumor invasion and metastasis. These results link TP63 and the basal gene expression program to ATDC and to aggressive tumor behavior. Defining ATDC as a molecular determinant of aggressive, basal cancers may lead to improved biomarkers and therapeutic approaches.

Keywords

Bladder cancer; ATDC; TRIM29; TP63; basal cancer

INTRODUCTION

In the United States, over 79 000 patients will be diagnosed with bladder cancer and >16 000 people will die this year¹. While noninvasive bladder cancers are common (80%) and often recur after resection, they rarely metastasize. In contrast, bladder tumors which display stromal and/or muscle-invasion (20%) frequently metastasize, even after aggressive multimodality therapy. Thus, a tumor's ability to invade through stroma (T1) and muscle (T2) is a defining feature of aggressive and lethal bladder cancers. Despite the clinical importance of this invasive phenotype, the biological factor(s) which govern invasive progression are poorly-defined.

Comprehensive profiling of human bladder cancers has revealed distinct molecular subtypes which correlate with clinical outcomes²⁻⁷. While there is variation in the definition and number of molecular subtypes, all classifications include both basal and luminal groups^{8,9}. The *luminal* subtype, which demonstrates a more differentiated gene signature with upregulation of genes like KRT20, GATA3 or PPAR γ , typically displays a more favorable prognosis. The *basal/squamous-like* subtype (BASQ-like), which is associated with a TP63-driven gene program, typically expresses high molecular weight keratins such as KRT5, KRT6, KRT14 and lack FOXA1 or GATA3 and portends a worse clinical prognosis. Other subcategories, including p53-like, urobasal A, urobasal B, infiltrative, genomically unstable and neuronal, each partly overlapping with basal or luminal subtyping have also been proposed^{7,9,10}. Molecular profiling of BASQ-like bladder tumors has determined that their molecular signature is similar to other types of human basal tumors, such as head and neck squamous cell carcinomas (HNSCC), non-small cell lung cancers and basal breast cancers, which are marked by upregulation of TP63 regulated genes, linking this entire family of aggressive, poor prognosis tumors¹¹.

TP63 has been proposed to be a regulator of the basal gene program but it exists in many isoforms which may possess distinct transcriptional activity^{11,12}. Specifically, TP63 has two alternate promoters/start sites which result in two distinct N terminal protein domains, TA (transactivation) or the dN domains. Both the TAp63 and dNp63 isoforms have α , β and γ splice variants in the carboxyl terminal region, resulting in multiple TP63 isoforms¹³.

Previously, dNp63 isoform expression was linked to basal cells in normal urothelium and to worse prognosis among patients with invasive bladder cancers¹⁴.

Ataxia Telangiectasia Group D Complementing (ATDC), also known as TRIM29, is an oncogene which promotes tumorigenesis in many organs^{15–18}. ATDC is highly expressed in human bladder cancers and overexpression is sufficient to drive bladder cancer development in transgenic (tg) mice¹⁶. ATDC expression also promotes invasion in pancreatic and bladder cancer cells^{16,19}. Nonetheless, it is rarely mutated or amplified in human cancers (cancer.sanger.ac.uk/cosmic/). While other groups have implicated miR-185 and -761 and ATM as mechanisms of ATDC expression modulation in other tumors, there is no evidence that expression of these molecules correlates with ATDC expression in human bladder cancers^{20–24}. Thus the factor(s) governing ATDC regulation in bladder cancer have not been clearly defined.

Here we demonstrate that ATDC expression is linked to TP63 expression and both are enriched in aggressive basal bladder cancers. We demonstrate that TP63 drives ATDC expression and binds directly to transcriptional enhancer sites within the first intron of ATDC using chromatin immunoprecipitation. TP63 expression also induces increased transcription of the basal gene KRT14 and together, ATDC and KRT14 promote basal bladder cancer cell invasion *in vivo* and *in vitro*. This work defines TP63 as a critical upstream regulator of ATDC, which serves to mediate an invasive basal gene program.

RESULTS

ATDC expression is highly correlated with expression of TP63 and basal genes.

ATDC is a driver of cancer formation and invasion but it is not commonly mutated or amplified^{15,16,18,19}. To identify genes which might regulate *ATDC* expression in cancer, we examined RNA-seq data from TCGA human urothelial carcinomas using the cBioPortal tool^{24,25}. Of the top 30 genes whose expression was most correlated with *ATDC* expression in human bladder cancer, only 3 were putative regulators of gene transcription and of these, only the tumor protein p63 (*TP63*, Spearman's R = 0.54, Pearson's R = 0.46, $p < 0.00001$, Table 1) has an established role in cancer biology. *TP63*, a paralog of p53, has been proposed as a transcriptional regulator of the basal gene program and is upregulated in basal subtype bladder, breast and ovarian cancers¹¹. Interestingly, expression of other basal genes, such as *KRT5* and *KRT6A* were also significantly correlated with *ATDC* expression in the TCGA bladder cancer data set (Table 1). Since *TP63*, *KRT5* and *KRT6A* are markers of aggressive BASQ-like bladder tumors which have poor prognosis, we decided to further interrogate the relationship of *TP63* and *ATDC* in basal subtype cancers.

To examine *ATDC*'s relationship to *TP63* and other genes associated with a basal molecular signature in human cancers, we compared expression of *ATDC*, *TP63*, *KRT14* and *KRT5*, in TCGA RNA sequencing data from multiple tumor types (Fig. 1a)^{24,25}. *ATDC* was significantly correlated with *TP63*, *KRT14* and *KRT5*, across multiple tumor types including bladder, breast, prostate and esophageal cancer (Fig. 1a; all p values < 0.0001).

ATDC is enriched in basal subtype bladder cancers.

TP63 and the basal keratins, *KRT14*, *KRT6* and *KRT5* are enriched in the aggressive BASQ-like subtype of bladder cancer⁷. To further explore the relationship between *ATDC* and basal subtype bladder cancers, we performed hierarchical clustering of 408 human bladder cancer specimens from TCGA using published luminal (*UPK1B*, *KRT20*, *UPK2*, *UPK3A*) and basal (*CD44*, *KRT14*, *KRT6B* and *KRT5*) marker genes (Fig. 1b)²⁻⁴. This analysis defined two clusters corresponding to basal (n = 117) and luminal (n=291) tumors and demonstrated that *TP63* and *ATDC* expression clustered with basal marker genes (Fig. 1b). To determine whether *ATDC* or *TP63* was upregulated in basal vs luminal subtypes, we next compared mRNA levels of each along with individual basal and luminal marker genes (Fig. 1c–d, Supplemental Fig. 1a–b). As expected, luminal tumors had higher expression of luminal marker genes and basal tumors had higher expression of basal marker genes (Supplemental Fig. 1). Both *ATDC* and *TP63* had significantly higher expression in basal vs luminal bladder cancers (Fig. 1c–d and Supplemental Fig. 1c, $p = 3.59 \times 10^{-22}$ and $p = 2.6 \times 10^{-21}$ respectively), demonstrating that *ATDC* mRNA expression is enriched in basal subtype tumors. Updated analysis of bladder cancers including the TCGA bladder cohort has further divided patients into five molecular subtypes; basal-squamous, luminal-papillary, luminal-infiltrated, luminal and neuronal^{9,10}. Using these subtype categories, we examined *ATDC* and *TP63* mRNA expression in the TCGA cohort and found that *ATDC* expression was highest in the basal-squamous subtype, lowest in the neuronal subtype and intermediate in the 3 luminal subtypes (Supplemental Fig. 2). Pair-wise Wilcoxon testing revealed significantly higher *ATDC* expression in basal-squamous vs luminal papillary, luminal and luminal-infiltrated subtypes ($p = 0.000542$) and in basal-squamous vs neuronal subtypes ($p = 0.0000154$). These results confirm that *ATDC* mRNA expression is enriched in the basal-squamous subtype of bladder cancer.

To determine if *ATDC* protein level was also elevated in basal bladder cancers, we performed immunohistochemical (IHC) staining of *ATDC*, *KRT14*, *KRT20* and *TP63* in 45 T2–T4 high-grade muscle invasive urothelial carcinomas. *ATDC* protein staining was enriched in samples with higher *TP63* and *KRT14* levels, whereas *ATDC* was lower in *KRT20*+ luminal tumors (representative images shown in Fig. 1e). To quantitate this difference, *ATDC* was scored based on intensity of IHC staining (0–3) in basal (*KRT14*+) and luminal (*KRT20*+) tumors and we found higher mean *ATDC* protein levels in basal vs luminal human bladder cancers (Figure 1f, $n = 45$, $p = 0.02$). These results indicate that *ATDC* protein level is significantly higher in basal subtype human bladder cancers.

dNp63 α expression is linked to *ATDC* and drives basal gene expression.

TP63 exists in many isoforms which may possess distinct transcriptional activity (Fig. 2a)^{11,12}. To examine which isoforms are expressed within basal and luminal human bladder cancers and understand their relationship with *ATDC*, we examined expression of each *TP63* isoform in the TCGA bladder cancer cohort and in 19 human bladder cancer cell lines^{26,27}. We found that the dNp63 N terminal isoforms were the most commonly expressed isoforms in both human TCGA specimens, representing 99% of total *TP63* expression (Fig. 2b) and in bladder cancer cell lines (Fig. 2c). All 3 of the major dNp63 C terminal variant isoforms were detected, with dNp63 α representing 71% of total *TP63* expressed in bladder cancer.

dNp63 α expression was 3 fold higher than the next most common isoform, dNp63 β ($p = 2.86 \times 10^{-27}$) (Fig. 2b and c). Further, dNp63 α , β and γ expression was significantly higher in basal as compared to luminal subtype tumors (Fig 2b). Although the TA forms of *TP63* were not detected in cell lines (Fig. 2c), TAp63 was detectable in a small subpopulation of human samples, representing less than 1% of all *TP63* present in the TCGA bladder cancer cohort (Fig. 2b). We next correlated expression of each individual isoform with *ATDC* expression using the TCGA bladder cancer dataset. Expression of all three dNp63 isoforms (α , β , γ) was highly correlated with *ATDC* mRNA expression (Fig. 2d).

To determine if dNp63 or TAp63 isoforms were capable of upregulating *ATDC*, we overexpressed both in UC10 and UC14 bladder cancer cell lines and measured the effect on *ATDC* expression. Ectopic expression of dNp63 α increased *ATDC* protein levels in both cell lines (Fig. 2e). While TAp63 α overexpression also increased *ATDC* levels to a lesser degree in both cell lines (Fig. 2e), we chose to focus on dNp63 α since it has previously been associated with regulation of aggressive basal gene programs¹¹ and poor patient outcomes^{14,28} and because the TAp63 isoforms are rarely expressed in human disease (Fig. 2b and c). To confirm that dNp63 α also promoted expression of *KRT14* and *KRT6A*, other genes associated with the basal signature, we measured their expression using qRT-PCR in our bladder cell lines with ectopic expression of dNp63 α and found that dNp63 α drives upregulation of these basal genes (Figs. 2f). Taken together, these results suggest that dNp63 α is the predominate isoform of *TP63* expressed in human bladder cancer and is a regulator *ATDC* expression in bladder cancer.

dNp63 α binds to an intronic enhancer of the *ATDC* gene.

If *TP63* is a transcriptional regulator of *ATDC*, then one would predict that it binds to regulatory DNA elements of *ATDC*. Chromatin immunoprecipitation of *TP63* combined with massive parallel sequencing (ChIP-seq) in human keratinocytes has revealed > 7500 putative *TP63* binding sites²⁹. To determine if *TP63* had putative binding sites within gene regulatory sequences of *ATDC* we downloaded this data set (GEO accession number GSE32061) and examined enriched sequences near the *ATDC* genomic locus using the UCSD genome browser (Fig. 3a)³⁰. We identified 3 regions enriched by *TP63* ChIP, all within the first intron of *ATDC* and corresponding to regions of known H3K27 acetylation indicative of transcriptional regulatory sites. These data suggest that *TP63* may be a direct transcriptional regulator of *ATDC* by binding to an intronic enhancer region of the gene.

To confirm that *TP63* binds these *ATDC* intronic sites in bladder cancer cell lines, we designed PCR primers to amplify DNA sequences corresponding to these three peaks (P1, P2 and P3 in Fig. 3a) and performed ChIP of *TP63* in UC14, UC5 (both with high endogenous *ATDC* and *TP63* expression and UC10 (low endogenous *ATDC* and *TP63* expression) bladder cancer cell lines with and without ectopic expression of dNp63 α . In UC14 (Fig. 3b), *TP63* ChIP enriched for the 3 putative *ATDC* intronic *TP63*-binding sites as well as a known *TP63* target gene, *CDKN1A*, but not negative controls (Satellite DNA or *RPL30*, a non-*TP63* target ribosomal gene). Ectopic expression of dNp63 α (dNp63 OE) did drive significantly increased *TP63* binding to *ATDC* intronic sites in UC14 which already has high endogenous *TP63* expression (Fig. 2e and 3b). Similar results were seen in the UC5

cell line which also harbors high endogenous levels of TP63 and ATDC (Fig. 3c). In UC10, no TP63 enrichment of *ATDC* intronic sequences was observed in control cell lines which have low endogenous TP63 expression, but ectopic overexpression of dNp63 α did increase TP63 ChIP of *ATDC* intronic sequences (Fig. 3d). The *KRT14* promoter is another known target of TP63 binding and regulation^{29,31}. To determine if TP63 ChIP also enriched *KRT14* promoter sequences in bladder cancer cell lines, we performed TP63 ChIP and found significant enrichment of the previously defined *KRT14* promoter site in UC10 and in UC14 cells with ectopic dNp63 α expression (Fig. 3e and f). Together these results demonstrate that TP63 binds directly to enhancer elements within the first intron of *ATDC* and the promoter of *KRT14*.

dNp63 α drives expression of ATDC.

Since TP63 expression was tightly correlated with ATDC expression and bound to regulatory sequences within the first intron, we hypothesized that TP63 was a transcriptional activator of *ATDC*. This was supported by ectopic expression of dNp63 α , in UC10 and UC14 driving upregulation of ATDC (Fig. 2e). Other groups have also implicated ATDC in regulation of TP63 in other tumor types³². To confirm that TP63 regulated ATDC expression and to determine if ATDC also regulated TP63 expression, we knocked down TP63 or ATDC in UC5 and UC14 bladder cancer cell lines. We observed that knockdown of TP63 decreased ATDC protein and mRNA, but ATDC knockdown had no effect on TP63 expression (Fig. 4a, b and c). To confirm that TP63 was a transcriptional activator of *ATDC* and *KRT14*, *ATDC* and *KRT14* reporter plasmids (tdTomato or GFP reporters, respectively) were co-transfected with empty vector or dNp63 α expression vectors into 253J (low endogenous TP63 expression) and UC5 (high endogenous TP63 expression) bladder cancer cell lines and fluorescence was measured. Overexpression of dNp63 α significantly increased *ATDC* and *KRT14* reporter expression (Supplemental Fig. 3). These results implicate TP63 as a specific transcriptional activator which drives increased expression of ATDC and KRT14.

KRT14 has previously been implicated in mediating basal cancer cell invasion and is directly regulated as part of the basal gene program induced by TP63^{4,11,33}. *KRT14* is upregulated in bladder cancer by TP63 and its expression is tightly correlated with *ATDC* expression in human bladder cancers (Figs. 1 and 2). Therefore, we next wanted to determine whether ATDC is required for TP63-mediated upregulation of *KRT14*. To measure this, we knocked down *ATDC* in cells with and without ectopic dNp63 α expression and measured expression of *TP63*, *ATDC* and *KRT14* mRNA using qRT-PCR in UC10 and UC14 cells (Fig. 4d–i). Ectopic overexpression of dNp63 α increased *TP63* mRNA levels by 100 fold in UC10 and 15 fold in UC14 while knock down of *ATDC* had no effect on *TP63* expression (Fig. 4d and e), suggesting that ATDC does not regulate *TP63* expression in bladder cancer cells. Ectopic overexpression of TP63 increased *ATDC* mRNA levels as expected in both cell lines (Fig. 4f and g). Ectopic overexpression of TP63 also promoted increased expression of *KRT14* mRNA and this increase was abrogated by knockdown of *ATDC* (Fig. 4h and i). To further confirm the specificity of these findings, we generated CRISPR-Cas9 mediated genomic knockout of *ATDC* in the UC14 cell line (Fig. 4j, l). Knockout of *ATDC* reduced expression of *KRT14* mRNA and protein but had no effect on

TP63 expression, similar to siRNA knockdown experiments (Fig. 4k, l). To confirm that ectopic *TP63* expression drove increased *ATDC* and *KRT14*, dNp63 α was overexpressed in UC14 *ATDC* wild type or KO cells and protein levels were measured by western blotting (Fig. 4l). *TP63* overexpression did increase *ATDC* and *KRT14* protein levels as expected (Fig. 4l and Supplemental Fig. 4). Similar results were obtained with UC5 cells (data not shown). These results suggest that *TP63* is an upstream regulator of both *ATDC* and *KRT14* and that *ATDC* regulates expression of *KRT14*.

dNp63 α induces invasion and proliferation via upregulation of *ATDC* and *KRT14*.

Knockdown of *ATDC* expression blocks invasion in bladder cancer cell lines¹⁶. Recent work has identified an important role for keratins in epithelial cell migration³⁴. Further, *TP63* and *KRT14* promote keratinocyte migration and breast cancer cell invasion^{33,35}. We therefore hypothesized that *TP63* drives an invasive phenotype via upregulation of *ATDC* and *KRT14*. To test this, we overexpressed dNp63 α or *ATDC* in human bladder cancer cell lines (253J, UC10 and UC14) and measured invasion using transwell assays. Overexpression of dNp63 α significantly increased invasion in all three bladder cancer cell lines (Fig. 5a–c). We also confirmed that overexpression of *ATDC* significantly increased invasion in the same bladder cancer cell lines, similar to what was previously observed (Fig. 5a–c)^{16,18,19,36}. To determine if *TP63*-induced invasion was dependent on expression of *ATDC* or *KRT14*, we next knocked down *ATDC*, *TP63* and *KRT14* in control cells and cells overexpressing dNp63 α . siRNA-mediated knockdown of *ATDC*, *TP63* and *KRT14* blocked *TP63*-induced invasion in both UC10 and UC14 cell lines (Fig. 5d and e). To further confirm that *ATDC* was required for *TP63*-induced invasion, we overexpressed dNp63 α in UC5 and UC14 bladder cancer cells with and without CRISPR-mediated *ATDC* knockout. We found that dNp63 α overexpression significantly increased transwell invasion, but that this *TP63*-driven invasion was blocked by *ATDC* KO (Fig. 5f and g).

We have previously shown that *ATDC* expression promotes cancer proliferation by effects on β -catenin and *PTEN*^{16,18}. To determine if dNp63 α also promoted proliferation and if *ATDC* and *KRT14* were required for this effect, we knocked down *ATDC* or *KRT14* using siRNA in UC14 bladder cancer cells expressing empty vector or dNp63 α . Overexpression of dNp63 α increased cell proliferation which was significantly reduced by knockdown of *ATDC* and *KRT14* (Supplemental Fig. 5).

Since the effect of dNp63 α on cancer cell proliferation could confound transwell invasion assays, we next interrogated the invasive phenotype induced by *ATDC* and *TP63* in a 3D tumor spheroid model system where cellular invasion and motility could be observed directly³⁷. In this system tumor spheroids (~ 50 μ m in diameter) were generated by culturing isogenic UC14 and UC5 bladder cancer cells with or without dNp63 α overexpression and CRISPR-mediated *ATDC* knockout in non-adherent conditions. We embedded the resulting tumor spheroids in type 1 collagen and monitored invasion using time-lapse microscopy for 72 hours. *ATDC* knockout blocked 3D tumor spheroid invasion and dNp63 α overexpression promoted more extensive invasion and migration at 72 hours (Fig. 5h–k, supplemental video). This effect was abrogated by *ATDC* knockout (Fig. 5h–k, supplemental video).

Together these results demonstrate that TP63 drives an invasive and proliferative program in basal bladder cancer and this program requires ATDC and KRT14.

dNp63 α promoted bladder tumor growth, invasion and metastasis *in vivo*.

We next sought to determine if TP63 promoted tumor growth and invasion *in vivo* and to define the contribution of ATDC to this behavior. Ectopic dNp63 α overexpression in UC10 and UC14 cells promoted tumor cell growth *in vivo* compared to control cells (Fig. 6a and b, Supplemental Fig. 6). H&E sections of these orthotopic bladder tumors demonstrated that dNp63 α overexpression drove significant muscle invasion for UC10 tumors, whereas control tumors did not demonstrate muscle invasion (Fig. 6c and d, Supplemental Fig. 6). To determine if ATDC expression was required for TP63-induced invasion and growth *in vivo*, we utilized isogenic UC14 cell lines with and without CRISPR-mediated ATDC knockout and ectopic expression of dNp63 α (OE) (Fig. 4l). Ectopic expression of dNp63 α promoted tumor growth and invasion compared to empty vector controls whereas ATDC knockout blocked TP63-promoted tumor growth ($p = 0.0025$ and 0.0173 respectively) (Fig. 6e and f, Supplemental Figure 7). To determine the impact of dNp63 α and ATDC on metastases *in vivo*, we inoculated bladders with luciferase labelled UC10 cells stably transduced with control or dNp63 α OE vector with or without shRNA knockdown of ATDC and tumor growth and metastasis was monitored using bioluminescence (Fig. 6g and h). dNp63 α OE resulted in larger tumors (Fig. 6g) and induced metastases (Fig. 6h, yellow arrows), an event not observed in control animals. Interestingly, shRNA-mediated knockdown of ATDC in the UC10 dNp63 α OE cells significantly reduced tumor growth and completely blocked metastatic spread (Fig. 6g and h). These results demonstrate that expression of dNp63 α promotes tumor growth, invasion and metastasis *in vivo* and that dNp63 α -induced metastasis is dependent on ATDC.

DISCUSSION

Patients with BASQ-like subtype bladder cancer typically have worse outcomes and shorter overall survival than other bladder cancer subtypes^{3,4,7,38}, but the molecular events driving this behavior are incompletely understood¹¹. Here we establish that TP63 directly regulates ATDC expression and mediates invasion in basal subtype bladder cancer using 3D invasion assays and orthotopic xenograft models. Since ATDC is rarely mutated or amplified in human cancers and the molecular events leading to increased expression have been incompletely defined, this data not only identifies ATDC as a novel mediator of basal tumor biology, but defines a new mechanism of expression regulation for this important oncogene. These results help to establish TP63, ATDC and KRT14 as an important regulators of the aggressive phenotype of basal tumors.

A TP63-regulated gene program has previously been proposed to be an important marker of basal tumor biology^{4,11,28}. The basal cytokeratins are proposed to play important roles in cell migration and invasion^{34,35}. Here we demonstrate that TP63 overexpression is sufficient to drive expression of ATDC and the basal intermediate filament gene, KRT14. Together, ATDC and KRT14 are required for invasion. Data from other tumor types has established that a basal gene program involving TP63 and KRT14 is employed in invasive leader cells of

breast cancer where these genes are selectively upregulated in the invading cancer cells and mediate invasive progression³³. Interestingly, *ATDC* is also upregulated in these invasive leader cells (personal communication, Andrew Ewald), suggesting that it is also linked to basal invasion programs in breast cancer and other cancer types. Therefore, this TP63-*ATDC* invasive axis appears to be conserved across basal subtype tumors suggesting that understanding this pathway has potential importance for many patients with diverse tumor types.

The observation that knockdown/knockout of *ATDC* negatively influenced KRT14 expression was potentially unexpected since TP63 was found to be a transcriptional activator and upstream of both genes (Figure 4). We have previously shown that *ATDC* functions by activation Wnt/ β -catenin signaling 16,18. Wnt/ β -catenin has recently be shown to upregulate KRT14 during cutaneous wound healing³⁹ suggesting that the effect of *ATDC* on KRT14 expression could be mediated through Wnt/ β -catenin signaling. In addition, *ATDC* has been previously shown to bind to, sequester and inhibit TP53⁴⁰ which itself has been shown to be a transcriptional repressor of KRT14⁴¹. Therefore, although TP63 is an upstream regulator of both *ATDC* and KRT14 transcription, multiple feedforward or backward mechanisms may exist linking *ATDC* to KRT14 transcriptional regulation and this may represent an area for future investigation.

TP63 is commonly expressed in bladder and other tumor types with basal squamous histology. Our analysis of *TP63* isoform expression in bladder cancers in TCGA and in bladder cancer cell lines represents a first comprehensive look at *TP63* isoform expression in this disease. We find that dNp63 α is the most highly expressed isoform (representing the vast majority of *TP63* transcripts in most bladder cancers) followed by the dNp63 β and γ isoforms. In contrast TAp63 isoforms are rarely expressed in human bladder cancers. It has previously been proposed that dNp63 and TAp63 isoform expression may correlate with patient outcomes and that dNp63 expression correlates with more aggressive disease in patients with muscle invasive bladder cancer^{14,28,42}, while others have suggested that dNp63 expressing tumors have a favorable prognosis⁴³. Our data supports the ability of dNp63 α to drive aggressive tumor behavior by upregulation of *ATDC* and promotion of tumor invasion and metastasis *in vitro* and *in vivo*. Interestingly, the TAp63 isoform was also able to upregulate *ATDC*, although to a lesser degree. Future work will be necessary to define how TAp63 and dNp63 isoforms interact in the rare cases where they are co-expressed in bladder cancers.

Given the poor clinical outcomes of patients with BASQ-like bladder cancers, it is essential to develop a better understanding of the pathways which drive their formation and progression. The identification of *ATDC* as a major driver of tumor formation¹⁶ and our findings here that TP63 regulates *ATDC* as a part of a basal gene program, establish an important linkage between TP63, *ATDC* and aggressive tumor biology. These data suggest that TP63 and *ATDC* are potential biomarkers of invasive progression, a critical determinant of outcome in patients with bladder cancer. Identification of TP63 and *ATDC* as drivers of basal tumor biology suggest a new therapeutically targetable pathway for patients who currently lack adequate treatment options.

Materials and Methods

Bioinformatic Analyses.

Description of RNA sequencing data sources, gene level and isoform expression analyses and molecular subtype analyses are available in Supplemental Material and Methods.

Cell Culture.

The bladder cancer cell lines UM-UC5, UC9, UC10, UC14, 253J were obtained from ATCC (253J) or Monica Liebert (UM-UC5, UC9, UC10, UC14), finger-printed, mycoplasma negative and passaged in DMEM with 10% serum as previously described¹⁶.

Tissue Microarray Construction and Immunohistochemistry.

Detailed information is described in Supplemental Material and Methods.

Generation of TP63 Overexpression Constructs.

Generation of TP63 Overexpression constructs is described in detail in Supplemental Material and Methods.

Immunoblot Analysis.

Immunoblot analysis was done as previously described¹⁸ and antibody information is available in Supplemental Material and Methods.

Quantitative RT-PCR.

Total RNA isolation, generation of cDNA and RT-PCR utilizing TaqMan Fast Universal PCR Master Mix was performed as previously described¹⁶ and information on probes is available in Supplemental Material and Methods. All reactions were performed in triplicate. mRNA expression was normalized to endogenous GAPDH.

Chromatin Immunoprecipitation.

All ChIP experiments were carried out using SimpleChIP Enzymatic Chromatin IP Kit (Cell Signaling Technology, Danvers, MA) according to kit protocol. Antibody and primer sequences are available in Supplemental Material and Methods.

siRNA Knockdowns and CRISPR-mediated ATDC Knockout.

Pre-designed SMART pool Ontarget plus siRNAs targeting TP63, ATDC, KRT14 and non-targeting controls were obtained from GE Dharmacon (Lafayette, CO) and transfected into cells using Lipofectamine RNAiMAX transfection reagent (ThermoFisher Scientific). ATDC knockout bladder cancer cell lines were generated using the Edit-R CRISPR-Cas9 system from Dharmacon (GE Healthcare, Lafayette, CO). Edit-R Lentiviral hEF1 α -Blast-Cas9 lentiviral particles were transduced into UM-UC5 and UC14 cells and stable Cas9 expressing line was generated by blasticidin selection. Cells were co-transfected with tracrRNA and ATDC-targeting crRNA (CR-012409-02-0005) specific for exon 1 or with non-targeting crRNA control (U-002000-05) all from Dharmacon. Individual colonies were

selected and screened for loss of ATDC expression and targeted mutations were confirmed using PCR and DNA sequencing.

Transwell invasion assays.

Invasion assays were performed using Collagen Cell Invasion Assays (ECM551) purchased from EMD Millipore (Darmstadt, Germany) and following manufacturer's instructions as previously described¹⁶.

3D invasion assays and imaging.

3D spheroid invasion assays were carried out as previously described.³⁷ Additional information is available in Supplemental Material and Methods.

Cell proliferation assays.

Cell proliferation was measured using the CellTiter-Glo Luminescent Cell Viability Assay (Promega, Madison, WI) and luminescence was read using a 96 well plate reader.

Orthotopic Bladder Tumor Models.

UC14 or UC10 bladder cancer cells (500,000) were injected into the bladder of each NSG mouse as previously described⁴⁴. Gender and ages (8–10 weeks old) were balanced between each group. Tumor formation and metastasis was monitored by palpation and bioluminescent imaging. Mice were sacrificed after 4–6 weeks depending on the cell line. Mouse bladders and internal organs were submitted for H&E and subsequent analysis. All animal experiments were in compliance with protocols approved by University Committee for the Use and Care of Animals (UCUCA) at the University of Michigan.

Statistics and General Methods.

Number of replicates per group (n) is presented in each figure and/or legend. Statistical tests used include t test, Wilcoxon and Mann-Whitney and are indicated in figure, legend or methods. Error bars are either standard deviation (S.D.) or standard error of the mean (S.E.M.) and are indicated for each figure. Center values are means unless indicated in legend. Each experiment was repeated independently at least twice. For the animal experiments, animals were excluded if they died prior to completion of study. Animal sample sizes were chosen based on experimental feasibility and no randomization or blinding was employed.

Supplementary Material

Refer to Web version on PubMed Central for supplementary material.

Acknowledgements:

Financial Support: This work was funded by grants from the University of Michigan Cancer Center Core Grant CA046592–26S3, NIH K08 CA201335 (PLP), BCAN YIA (PLP), ASCO YIA (PLP), NIH R01 CA17483601 (DMS).

The authors would like to thank Andrew Ewald for assistance with the 3D invasion and imaging systems used in this study. The authors declare no competing financial interests.

REFERENCES

1. Siegel RL, Miller KD & Jemal A Cancer statistics, 2016. *CA Cancer J Clin* 66, 7–30, doi:10.3322/caac.21332 (2016). [PubMed: 26742998]
2. Network TCGAR Comprehensive molecular characterization of urothelial bladder carcinoma. *Nature*, doi:10.1038/nature12965 (2014).
3. Damrauer JS et al. Intrinsic subtypes of high-grade bladder cancer reflect the hallmarks of breast cancer biology. *Proc Natl Acad Sci U S A* 111, 3110–3115, doi:10.1073/pnas.1318376111 (2014). [PubMed: 24520177]
4. Choi W et al. Identification of distinct basal and luminal subtypes of muscle-invasive bladder cancer with different sensitivities to frontline chemotherapy. *Cancer Cell* 25, 152–165, doi:10.1016/j.ccr.2014.01.009 (2014). [PubMed: 24525232]
5. Hedegaard J et al. Comprehensive Transcriptional Analysis of Early-Stage Urothelial Carcinoma. *Cancer Cell* 30, 27–42, doi:10.1016/j.ccell.2016.05.004 (2016). [PubMed: 27321955]
6. Sjö Dahl G et al. A molecular taxonomy for urothelial carcinoma. *Clin Cancer Res* 18, 3377–3386, doi:10.1158/1078-0432.CCR-12-0077-T (2012). [PubMed: 22553347]
7. Lerner SP et al. Bladder Cancer Molecular Taxonomy: Summary from a Consensus Meeting. *Bladder Cancer* 2, 37–47, doi:10.3233/BLC-150037 (2016). [PubMed: 27376123]
8. Choi W et al. Genetic Alterations in the Molecular Subtypes of Bladder Cancer: Illustration in the Cancer Genome Atlas Dataset. *Eur Urol* 72, 354–365, doi:10.1016/j.eururo.2017.03.010 (2017). [PubMed: 28365159]
9. Robertson AG et al. Comprehensive Molecular Characterization of Muscle-Invasive Bladder Cancer. *Cell* 171, 540–556.e525, doi:10.1016/j.cell.2017.09.007 (2017). [PubMed: 28988769]
10. Sjö Dahl G, Eriksson P, Liedberg F & Hoglund M Molecular classification of urothelial carcinoma: global mRNA classification versus tumour-cell phenotype classification. *J Pathol* 242, 113–125, doi:10.1002/path.4886 (2017). [PubMed: 28195647]
11. Hoadley KA et al. Multiplatform Analysis of 12 Cancer Types Reveals Molecular Classification within and across Tissues of Origin. *Cell* 158, 929–944, doi:10.1016/j.cell.2014.06.049 (2014). [PubMed: 25109877]
12. Murray-Zmijewski F, Lane DP & Bourdon JC p53/p63/p73 isoforms: an orchestra of isoforms to harmonise cell differentiation and response to stress. *Cell Death Differ* 13, 962–972, doi:10.1038/sj.cdd.4401914 (2006). [PubMed: 16601753]
13. Su X, Chakravarti D & Flores ER p63 steps into the limelight: crucial roles in the suppression of tumorigenesis and metastasis. *Nat Rev Cancer* 13, 136–143, doi:10.1038/nrc3446 (2013). [PubMed: 23344544]
14. Karni-Schmidt O et al. Distinct expression profiles of p63 variants during urothelial development and bladder cancer progression. *Am J Pathol* 178, 1350–1360, doi:10.1016/j.ajpath.2010.11.061 (2011). [PubMed: 21356385]
15. Lai W et al. Upregulated ataxia-telangiectasia group D complementing gene correlates with poor prognosis in patients with esophageal squamous cell carcinoma. *Dis Esophagus* 26, 817–822, doi:10.1111/j.1442-2050.2012.01400.x (2013). [PubMed: 23020249]
16. Palmboos PL et al. ATDC/TRIM29 Drives Invasive Bladder Cancer Formation through miRNA-Mediated and Epigenetic Mechanisms. *Cancer Res* 75, 5155–5166, doi:10.1158/0008-5472.CAN-15-0603 (2015). [PubMed: 26471361]
17. Tang ZP et al. Ataxia-Telangiectasia Group D Complementing Gene (ATDC) Promotes Lung Cancer Cell Proliferation by Activating NF- κ B Pathway. *PLoS One* 8, e63676, doi:10.1371/journal.pone.0063676 (2013). [PubMed: 23776433]
18. Wang L et al. Oncogenic function of ATDC in pancreatic cancer through Wnt pathway activation and beta-catenin stabilization. *Cancer Cell* 15, 207–219, doi:10.1016/j.ccr.2009.01.018 (2009). [PubMed: 19249679]
19. Wang L et al. ATDC induces an invasive switch in KRAS-induced pancreatic tumorigenesis. *Genes Dev* 29, 171–183, doi:10.1101/gad.253591.114 (2015). [PubMed: 25593307]
20. Qiu F, Xiong JP, Deng J & Xiang XJ TRIM29 functions as an oncogene in gastric cancer and is regulated by miR-185. *Int J Clin Exp Pathol* 8, 5053–5061 (2015). [PubMed: 26191199]

21. Dükel M et al. The Breast Cancer Tumor Suppressor TRIM29 Is Expressed via ATM-dependent Signaling in Response to Hypoxia. *J Biol Chem* 291, 21541–21552, doi:10.1074/jbc.M116.730960 (2016). [PubMed: 27535224]
22. Guo GC, Wang JX, Han ML, Zhang LP & Li L microRNA-761 induces aggressive phenotypes in triple-negative breast cancer cells by repressing TRIM29 expression. *Cell Oncol (Dordr)* 40, 157–166, doi:10.1007/s13402-016-0312-6 (2017). [PubMed: 28054302]
23. Guo G et al. Whole-genome and whole-exome sequencing of bladder cancer identifies frequent alterations in genes involved in sister chromatid cohesion and segregation. *Nat Genet*, doi: 10.1038/ng.2798 (2013).
24. Cerami E et al. The cBio cancer genomics portal: an open platform for exploring multidimensional cancer genomics data. *Cancer Discov* 2, 401–404, doi:10.1158/2159-8290.CD-12-0095 (2012). [PubMed: 22588877]
25. Gao J et al. Integrative analysis of complex cancer genomics and clinical profiles using the cBioPortal. *Sci Signal* 6, pii, doi:10.1126/scisignal.2004088 (2013).
26. Tamura S et al. Molecular correlates of in vitro responses to dacomitinib and afatinib in bladder cancer. *Bladder Cancer* (2017).
27. Hovelson DH et al. Targeted DNA and RNA Sequencing of Paired Urothelial and Squamous Bladder Cancers Reveals Discordant Genomic and Transcriptomic Events and Unique Therapeutic Implications. *Eur Urol*, doi:10.1016/j.eururo.2018.06.047 (2018).
28. Choi W et al. p63 expression defines a lethal subset of muscle-invasive bladder cancers. *PLoS One* 7, e30206, doi:10.1371/journal.pone.0030206 (2012). [PubMed: 22253920]
29. McDade SS et al. Genome-wide analysis of p63 binding sites identifies AP-2 factors as co-regulators of epidermal differentiation. *Nucleic Acids Res* 40, 7190–7206, doi:10.1093/nar/gks389 (2012). [PubMed: 22573176]
30. Kent WJ et al. The human genome browser at UCSC. *Genome Res* 12, 996–1006, doi:10.1101/gr.229102. Article published online before print in May 2002 (2002). [PubMed: 12045153]
31. Candi E et al. Differential roles of p63 isoforms in epidermal development: selective genetic complementation in p63 null mice. *Cell Death Differ* 13, 1037–1047, doi:10.1038/sj.cdd.4401926 (2006). [PubMed: 16601749]
32. Masuda Y, Takahashi H & Hatakeyama S TRIM29 regulates the p63-mediated pathway in cervical cancer cells. *Biochim Biophys Acta* 1853, 2296–2305, doi:10.1016/j.bbamcr.2015.05.035 (2015). [PubMed: 26071105]
33. Cheung KJ, Gabrielson E, Werb Z & Ewald AJ Collective invasion in breast cancer requires a conserved basal epithelial program. *Cell* 155, 1639–1651, doi:10.1016/j.cell.2013.11.029 (2013). [PubMed: 24332913]
34. Wang F, Chen S, Liu HB, Parent CA & Coulombe PA Keratin 6 regulates collective keratinocyte migration by altering cell-cell and cell-matrix adhesion. *J Cell Biol*, doi:10.1083/jcb.201712130 (2018).
35. Velez-delValle C, Marsch-Moreno M, Castro-Munozledo F, Galvan-Mendoza IJ & Kuri-Harcuch W Epithelial cell migration requires the interaction between the vimentin and keratin intermediate filaments. *Sci Rep* 6, 24389, doi:10.1038/srep24389 (2016). [PubMed: 27072292]
36. Xu W et al. RNA interference against TRIM29 inhibits migration and invasion of colorectal cancer cells. *Oncol Rep* 36, 1411–1418, doi:10.3892/or.2016.4941 (2016). [PubMed: 27430345]
37. Wang Y, Day ML, Simeone DM & Palmboos PL 3-D Cell Culture System for Studying Invasion and Evaluating Therapeutics in Bladder Cancer. *J Vis Exp In Press*, doi:10.3791/58345 (2018).
38. Seiler R et al. Impact of Molecular Subtypes in Muscle-invasive Bladder Cancer on Predicting Response and Survival after Neoadjuvant Chemotherapy. *Eur Urol*, doi:10.1016/j.eururo.2017.03.030 (2017).
39. Lee SH et al. The Dishevelled-binding protein CXXC5 negatively regulates cutaneous wound healing. *J Exp Med* 212, 1061–1080, doi:10.1084/jem.20141601 (2015). [PubMed: 26056233]
40. Yuan Z et al. The ATDC (TRIM29) protein binds p53 and antagonizes p53-mediated functions. *Mol Cell Biol* 30, 3004–3015, doi:MCB.01023-09 [pii](2010). [PubMed: 20368352]

41. Cai BH et al. p53 acts as a co-repressor to regulate keratin 14 expression during epidermal cell differentiation. *PLoS One* 7, e41742, doi:10.1371/journal.pone.0041742 (2012). [PubMed: 22911849]
42. Leivo MZ, Elson PJ, Tacha DE, Delahunt B & Hansel DE A combination of p40, GATA-3 and uroplakin II shows utility in the diagnosis and prognosis of muscle-invasive urothelial carcinoma. *Pathology* 48, 543–549, doi:10.1016/j.pathol.2016.05.008 (2016). [PubMed: 27594510]
43. Gaya JM et al. Np63 expression is a protective factor of progression in clinical high grade T1 bladder cancer. *J Urol* 193, 1144–1150, doi:10.1016/j.juro.2014.10.098 (2015). [PubMed: 25444981]
44. Han AL et al. Fibulin-3 promotes muscle-invasive bladder cancer. *Oncogene*, doi:10.1038/onc.2017.149 (2017).

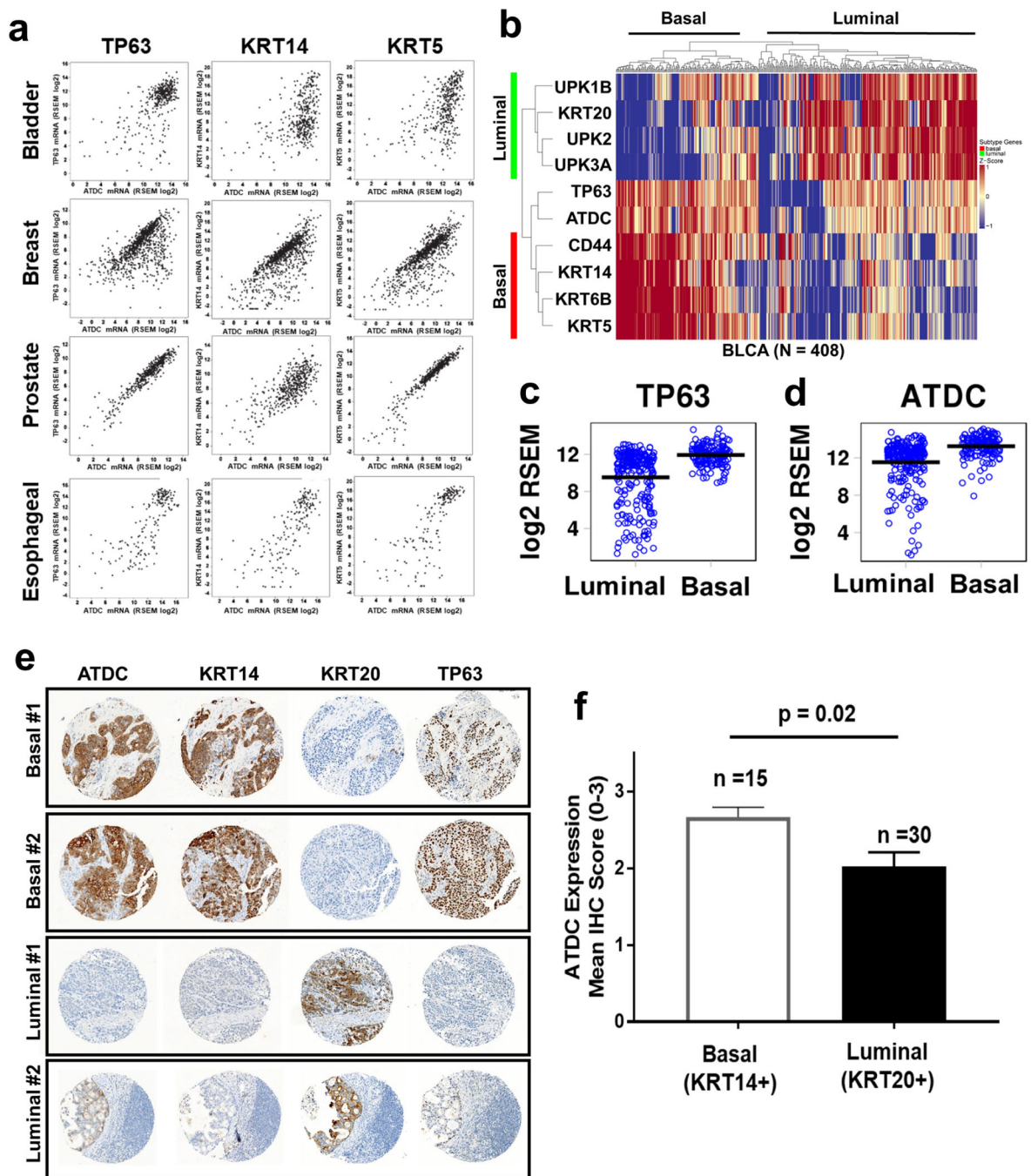


Fig. 1. *ATDC* is correlated with *TP63* and basal gene expression and is enriched in basal subtype bladder cancers. (a) *ATDC* is correlated with *TP63*, *KRT14* and *KRT5* mRNA levels in bladder, breast, prostate and esophageal cancers based on analysis of TCGA data. Pearson and Spearman correlations with *ATDC*: Bladder (n=413): *TP63* (0.46, 0.54), *KRT14* (0.34, 0.42), *KRT5* (0.5, 0.52). Breast (n=1105): *TP63* (0.43, 0.56), *KRT14* (0.49, 0.74), *KRT5* (0.5, 0.79). Prostate (n=499): *TP63* (0.88, 0.94), *KRT14* (0.4, 0.69), *KRT5* (0.93, 0.97). Esophageal (n=185): *TP63* (0.41, 0.77), *KRT14* (0.47, 0.79), *KRT5* (0.72, 0.85). p-values for

all Pearson correlations are < 0.00001 . (b) Hierarchical clustering analysis of basal and luminal gene expression in TCGA human bladder cancers demonstrates that ATDC and TP63 expression is most closely associated with basal subtype bladder cancer. Heatmap was generated using z-scores calculated per-gene across all patients. (c-d) Scatter plots representing *TP63* and *ATDC* expression in the luminal or basal tumors identified in Fig 1b. Line represents mean log₂ RSEM expression. Expression differences between luminal and basal subtypes were highly statistically significant: *ATDC* $p = 3.59 \times 10^{-22}$ and *TP63* $p = 2.6 \times 10^{-21}$. (e) Immunohistochemical staining for ATDC, KRT14, KRT20 and TP63 in human muscle invasive bladder cancer samples demonstrates ATDC co-expression in representative tumors with basal marker expression (top 2 panels), but not in luminal tumors expressing the marker KRT20 (bottom 2 panels). (f) Bar graph showing ATDC protein expression as measured by IHC in basal (KRT14+, n = 15) and luminal (KRT20+, n = 30) human bladder tumors. Expression of ATDC was scored 0 (no staining) to 3 (intense staining) by experience observer blinded to experimental conditions. Student t test p value = 0.02. Error bars = SEM.

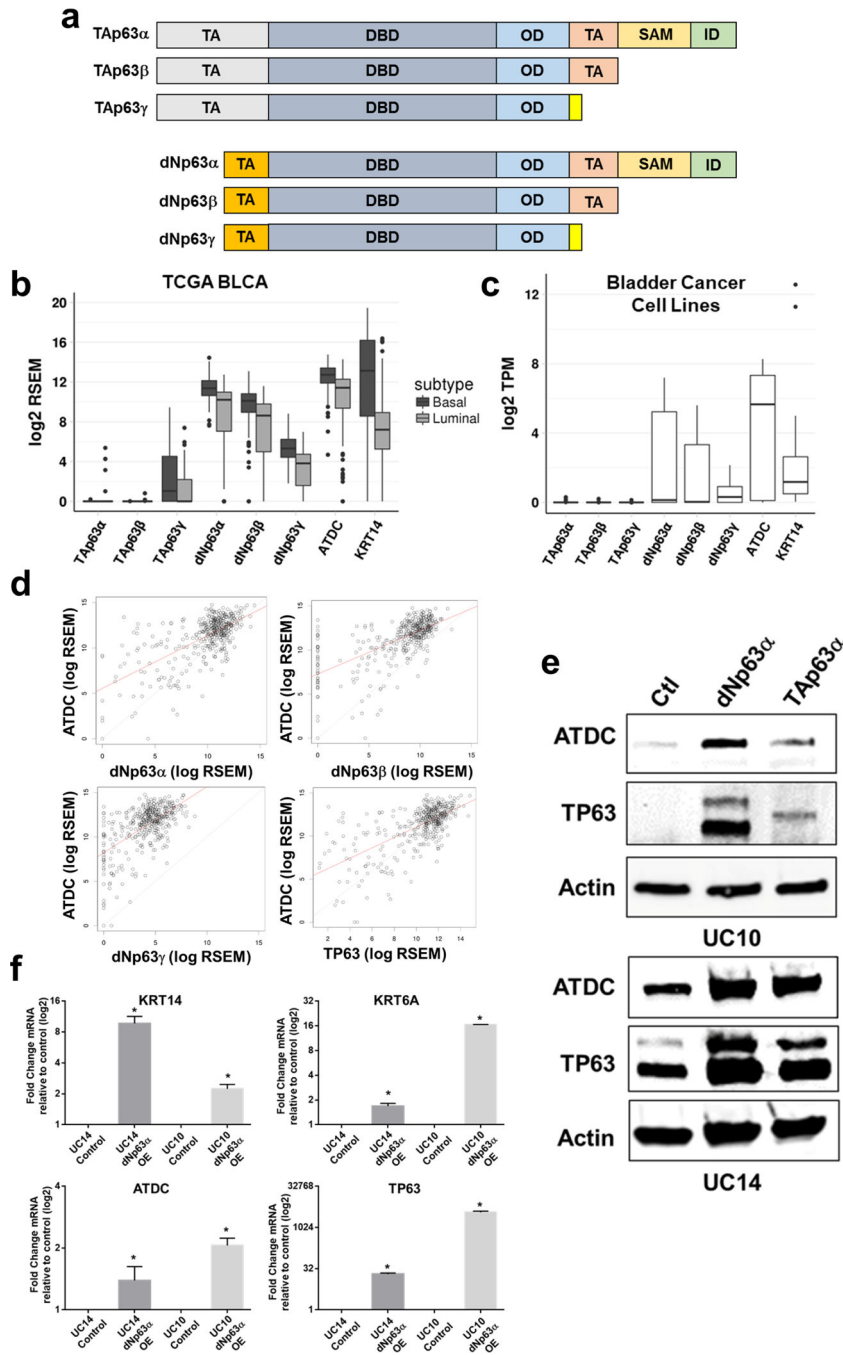


Fig. 2. dNp63 α is the most commonly expressed isoform of TP63 in bladder cancer and drives ATDC and basal gene expression. (a) Schematic diagram of TP63 isoforms. (b) Analysis of TCGA RNA sequencing data from bladder cancer samples (BLCA) classified as basal or luminal subtype demonstrates that dNp63 α is predominate isoform expressed in human bladder cancer followed by dNp63 β and dNp63 γ respectively. dNp63 α , β and γ were all more highly expressed in basal vs luminal subtypes (5.65 fold increase, $p = 8 \times 10^{-22}$; 6.06 fold increase, $p = 2.3 \times 10^{-17}$; 4.1 fold increase, $p = 1.7 \times 10^{-24}$ respectively). (c) Similar

TP63 isoform expression patterns were observed in a panel of 20 human bladder cancer cell lines. Line indicates median and box indicates first-third interquartile range for (b-c). (d) ATDC expression is significantly correlated with expression of dNp63 α (Pearson 0.659), dNp63 β (Pearson 0.662) and dNp63 γ (Pearson 0.600) as well as total TP63 (Pearson 0.655) in the bladder cancer TCGA data set (all p values < 0.0001). (e) Overexpression of dNp63 α and TAp63 α drives upregulation of ATDC expression in UC10 and UC14 bladder cancer cell lines as measured by western blotting. (f) Overexpression of dNp63 α in UC14 and UC10 human bladder cancer cell lines promoted expression of KRT14 and KRT6A genes as well as ATDC as measured by quantitative RT-PCR. n = 3 for each condition. Error bars = S.D. * indicates p < 0.05 compared to controls.

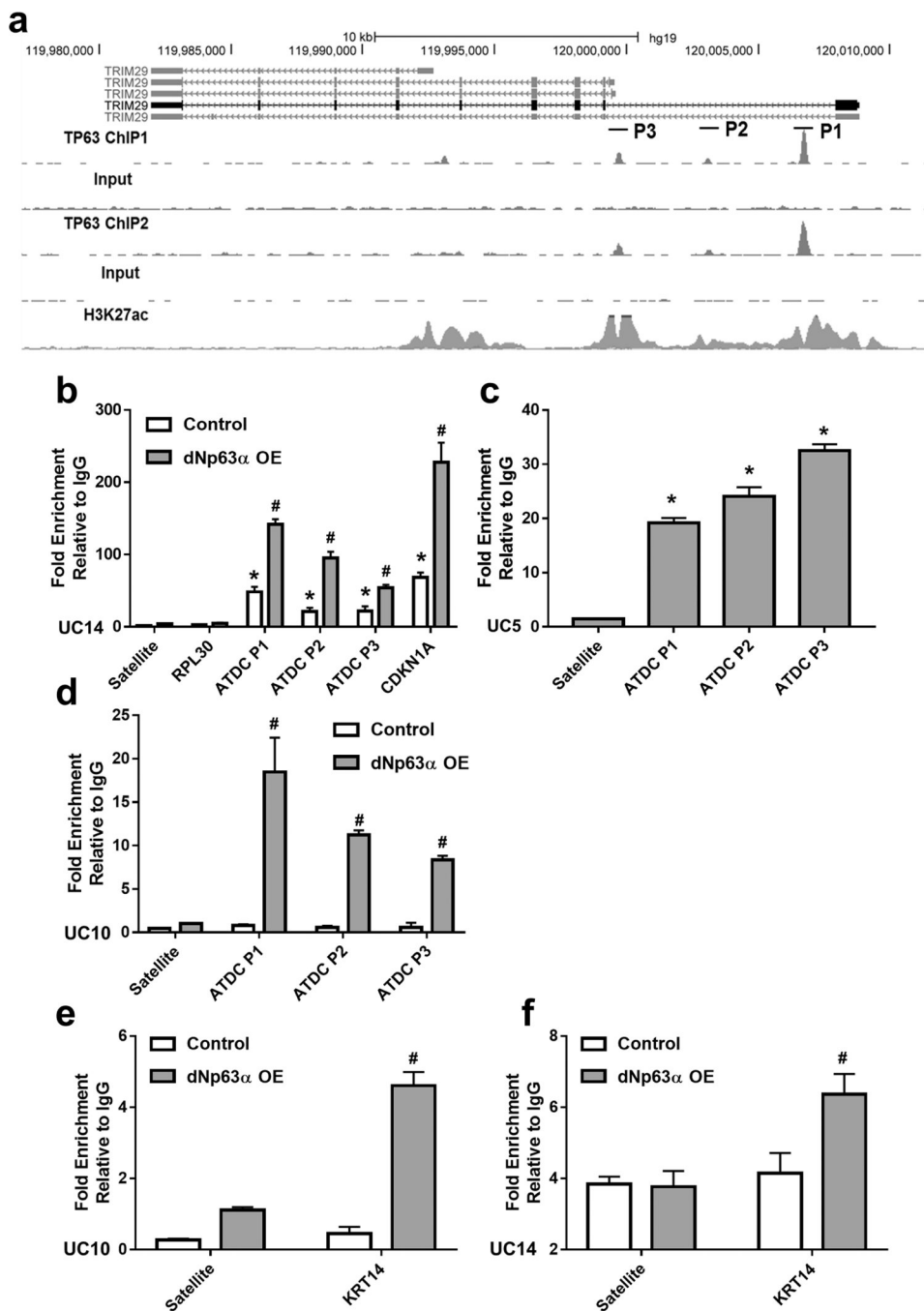


Fig. 3. TP63 binds to ATDC enhancer and KRT14 promoter elements. (a) TP63 chromatin immunoprecipitation (ChIP) sequencing data from human keratinocytes (GEO accession number GSE32061) identifies 3 putative TP63 binding sites within ATDC enhancer. Putative TP63 binding sites correspond to transcriptionally active regions marked by H3K27 acetylation. P1, P2 and P3 refer to location of PCR products used in (b-d). (b) ChIP of TP63 (p63α IP) in the UC14 bladder cancer cell line transduced with control or dNp63α overexpression (dNp63α OE) vectors indicates enrichment of ATDC P1, P2 and P3

sequence compared to IgG controls. dNp63 α overexpression increased TP63 occupancy of binding sites in UC14. CDKN1A is a positive control target of TP63 binding. Satellite and RPL30 are negative controls. (c) TP63 ChIP in UC5 bladder cancer cell line confirms TP63 occupancy on ATDC P1, 2 and 3 binding sites. (d) TP63 ChIP in UC10 bladder cancer cells (low endogenous TP63 and ATDC) with and without ectopic dNp63 α expression demonstrates TP63 occupancy at ATDC promoter sites only in cells with ectopic dNp63 α expression. (e and f) TP63 ChIP in UC10 and UC14 cells with ectopic dNp63 α demonstrates enrichment of KRT14 promoter element. All samples are done in triplicate. Error Bars = S.D. * denotes a statistically significant difference ($p < 0.05$, student t test) compared to satellite negative control for all panels. # denotes a statistically significant difference ($p < 0.05$, student t test) compared to both satellite negative control and vector control conditions for all panels.

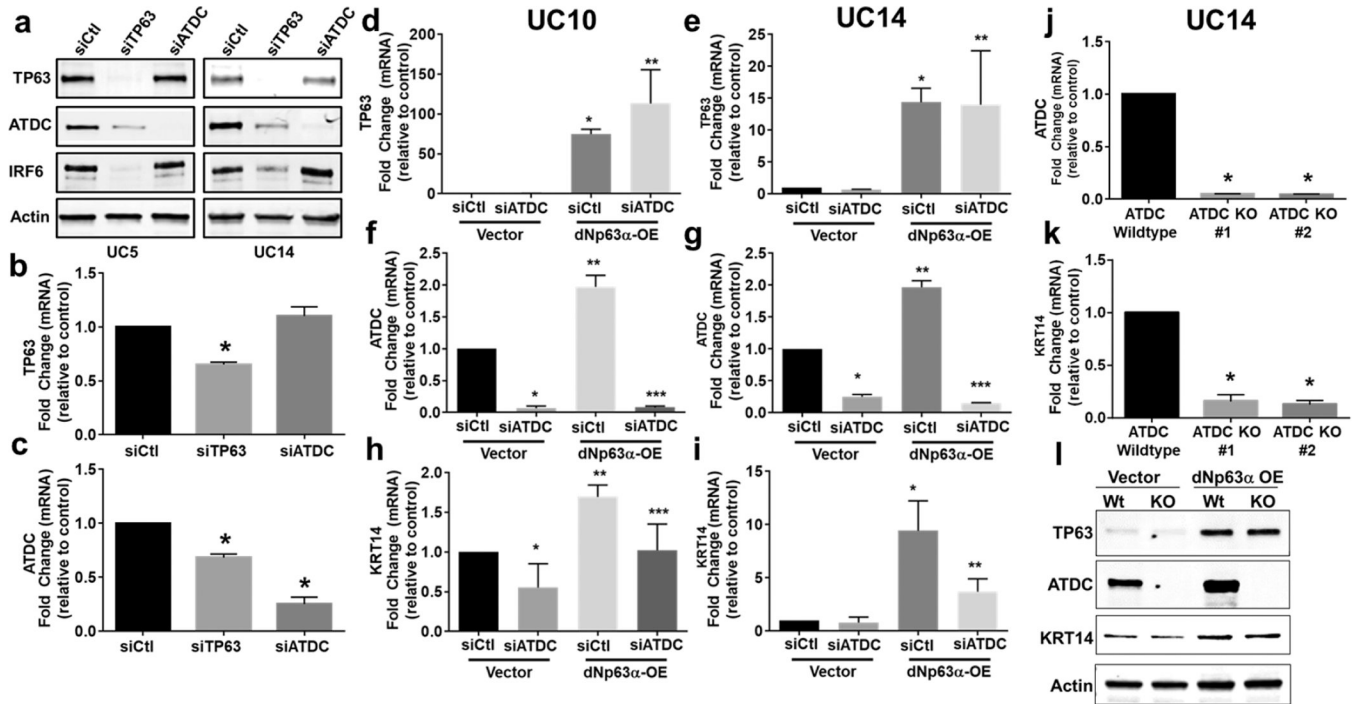


Fig. 4. TP63 Drives Expression of ATDC and KRT14 in Bladder Cancer. (a) siRNA-mediated knockdown of TP63 reduced ATDC expression in UC5 and UC14 bladder cancer cell lines, but siRNA-mediated knockdown of ATDC had no effect on TP63 expression as measured by western blotting. IRF6 serves as a known TP63 target control. (b and c) siRNA-mediated knockdown of TP63 reduces *TP63* and *ATDC* mRNA expression as measured by qRT-PCR in UC14. Error Bar = S.D. * $p < 0.0001$ compared to siCtrl (d-e) Overexpression of dNp63 α (dNp63 α -OE) in UC10 (d) and UC14 (e) promotes increased expression of *TP63* mRNA (qRT-PCR) compared to empty vector control (Vector) which was not effected by knockdown of ATDC with siRNA. Error Bar = S.D. N = 3. * $p < 0.0001$, ** $p = 0.0099$ compared to Vector siCtrl for (d). * $p = 0.0005$, ** $p = 0.05$, each compared to Vector siCtrl for (e). (f-g) dNp63 α -OE upregulated expression of *ATDC* mRNA (dNp63 α -OE siCtrl compared to Vector siCtrl) in UC10 (f) and UC14 (g). Error Bar = S.D. N = 3. * $p < 0.0001$ compared to Vector siCtrl, ** $p = 0.0007$ compared to Vector siCtrl, *** $p < 0.0001$ compared to dNp63 α -OE siCtrl for (f). * $p < 0.0001$ compared to Vector siCtrl, ** $p < 0.0001$ compared to Vector siCtrl, *** $p = 0.0001$ each compared to dNp63 α -OE siCtrl for (g). (h-i) dNp63 α -OE upregulated expression of *KRT14* mRNA (dNp63 α -OE siCtrl compared to Vector siCtrl) but this upregulation was reduced by ATDC siRNA mediated KD (dNp63 α -OE siCtrl compared to dNp63 α -OE siATDC) in UC10 (h) and UC14 (i). Error Bar = S.D. N = 3. * $p = 0.06$ compared to Vector siCtrl, ** $p = 0.0012$ compared to Vector siCtrl, *** $p = 0.03$ compared to dNp63 α -OE siCtrl for (h). * $p = 0.007$ compared to Vector siCtrl, ** $p = 0.0313$ compared to dNp63 α -OE siCtrl for (i). (j) CRISPR-Cas9 mediated genomic ablation of ATDC in UC14 (ATDC Knockout #1 and 2) results in loss of *ATDC* mRNA. Error Bars = S.D. n = 3. * $p < 0.0001$ compared to ATDC wild type. (k) ATDC Knockout results in significant decrease in *KRT14* mRNA expression. Error Bars = S.D. n = 3. * $p < 0.001$

compared to wild type. (l) UC14 ATDC knockout (KO) cells have reduced ATDC and KRT14 protein expression compared to ATDC wild type (Wt). dNp63 α -OE increased ATDC and KRT14 expression.

Author Manuscript

Author Manuscript

Author Manuscript

Author Manuscript

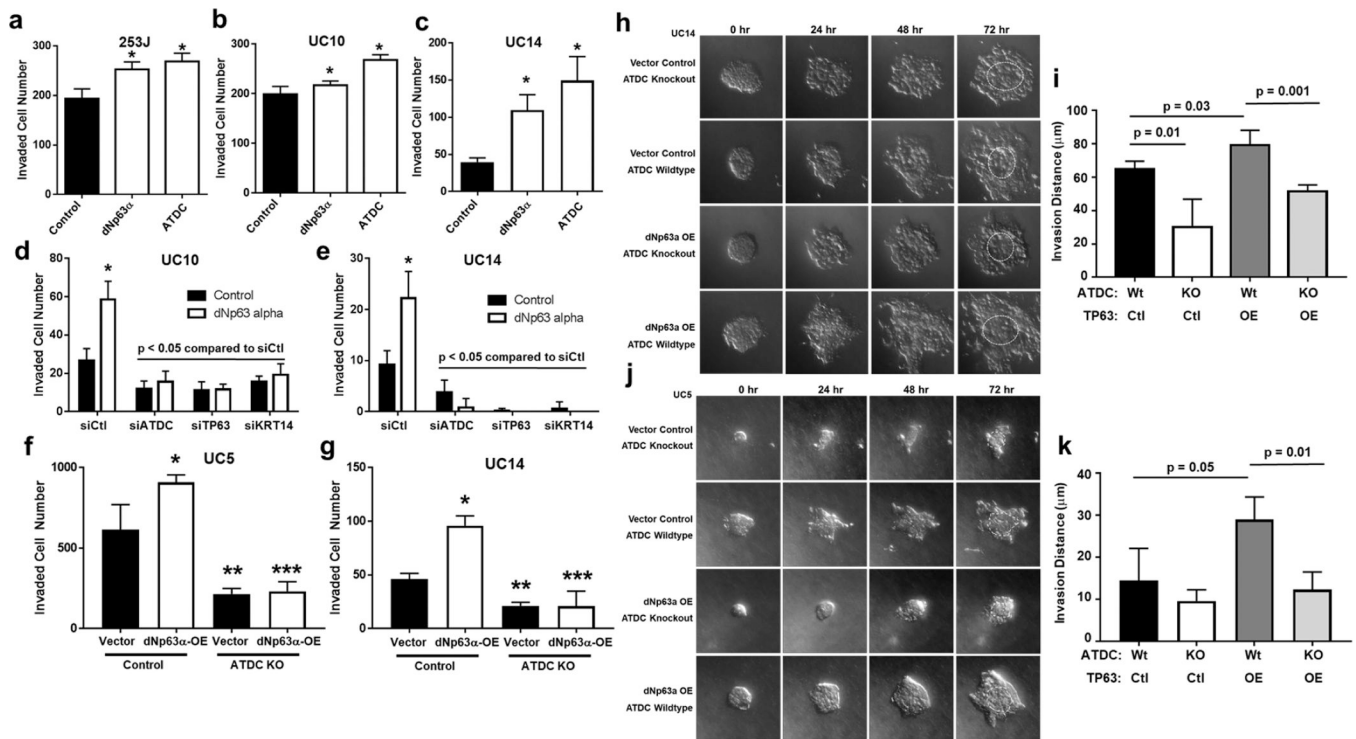


Fig. 5. TP63 promotes invasion and requires ATDC and KRT14. Overexpression of dNp63α or ATDC drives increased invasion as measured by transwell assays for 253J (a), UC10 (b) or UC14 (c). n = 5. Error Bars = S.D. * p < 0.05 compared to control. (d-e) siRNA-mediated KD of ATDC and KRT14 blocked dNp63α induced invasion in transwell assays in UC10 (d) and UC14 (e). n = 4. Error Bars = S.D. * p < 0.05 compared to control. (f and g) dNp63α overexpression (OE) in UC5 (f) and UC14 (g) bladder cancer cells promoted invasion which was blocked by ATDC knockout. n = 3. Error Bars = S.D. * p < 0.05 compared to vector control. ** and *** p < 0.05 compared to dNp63α control. (h-k) dNp63α overexpression promoted invasion in 3D tumor spheroid invasion assays using UC14 (h) and UC5 (j) and this effect was blocked by ATDC knockout. Circles indicate extent of tumor prior to invasion. (i and k) Quantification of linear invasion distance of tumor spheroids shown in (h and j). Graphs shows mean of 4 independent measurements of farthest invaded distance. Error Bars = S.D.

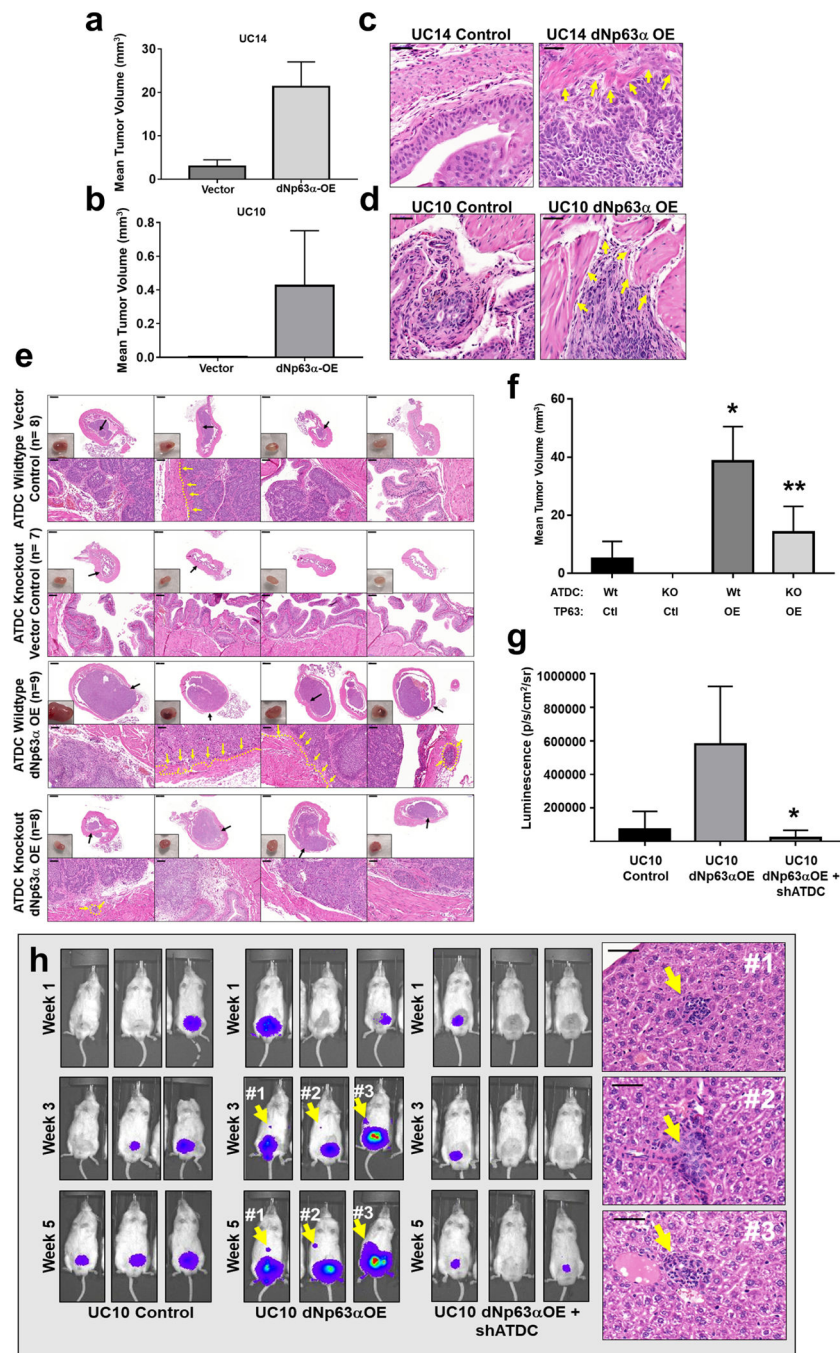


Fig. 6. TP63 drives *in vivo* tumor growth and invasion and requires ATDC. TP63 overexpression in UC14 (a) and UC10 (b) increased tumor growth in bladder orthotopic models. UC14 control vs dNp63 α OE p value = 0.0053. UC10 control vs dNp63 α OE p value = 0.21. n = 8–14 animals per group. Error bars = S.E.M. (c-d) H&E images of orthotopic UC14 (c) and UC10 (d) bladder tumors demonstrate increased invasion in tumors with dNp63 α -OE. Arrows indicate areas of tumor invasion into the muscularis propria. Bar = 50 μ m. (e) Knockout of ATDC blocks TP63 induced tumor growth and invasion in an orthotopic bladder tumor

model (UC14 cells) at 4 weeks. Four representative tumor bearing mouse bladders are shown. Upper panels show 2× cross-sectional H&E image of bladder plus tumor (Bar = 500µm). Black arrows indicate tumor. Inset image of corresponding bladder from necropsy. Lower panels show 20× H&E image of bladder tumor (Bar = 50µm). Yellow arrows and dashed line indicate muscle invasion. (f) Quantitation of tumor volumes from (e). Wt = ATDC wildtype. KO = ATDC knockout. Ctl = empty control overexpression vector. OE = dNp63α overexpression. * p = 0.0025 compared to ATDC Wt, TP63 Vector Ctl. ** p = 0.0173 compared to ATDC Wt, TP63 OE. Error bars = S.E.M. (g) Quantification of luciferase activity of bioluminescent primary bladder tumors demonstrated that knock down of ATDC (shATDC) blocked TP63-induced tumor growth of UC10 orthotopic tumors. Error bars = S.E.M. * p = 0.03 compared to UC10 dNp63α.OE. (h) Knock down of ATDC (shATDC) blocked TP63-induced metastases from UC10 orthotopic tumors (Control n = 10, dNp63α.OE n = 8 and dNp63α.OE+shATDC n = 10). Bioluminescent imaging of 3 representative mice from each group are shown 1, 3 and 5 weeks after inoculation of bladder. Numbers and arrows indicate liver metastases confirmed by serial bioluminescent imaging, necropsy and H&E. Numbered H&E images of liver metastases shown on the right match numbered bioluminescent images. Bar = 50µm.

Table 1.

Genes with highest correlation with ATDC mRNA expression in TCGA bladder urothelial carcinoma samples.

| Gene | Pearson's Correlation | Spearman's Correlation | Gene Description |
|----------|-----------------------|------------------------|--|
| PVRL1 | 0.67 | 0.71 | Nectin1. Ca++ independent cell-cell adhesion. |
| GJB5 | 0.6 | 0.67 | Gap junction protein beta 5. Connexin family. |
| PERP | 0.58 | 0.61 | TP53 apoptosis effector. Desmosome. |
| JUP | 0.55 | 0.55 | Junction plakoglobin. Desmosome, intermediate junctions. |
| FAT2 | 0.53 | 0.6 | FAT atypical cadherin 2 |
| SFN | 0.52 | 0.54 | Stratifin. Cell cycle checkpoint. |
| GJB3 | 0.51 | 0.57 | Gap junction protein beta 3. Connexin family. |
| LYPD3 | 0.5 | 0.61 | Ly6/PLAUR domain containing 3. |
| PKP1 | 0.5 | 0.6 | Plakophilini. Desmosome/nuclei. |
| KRT5 | 0.5 | 0.52 | Keratin 5. Basal type II cytokeratin. Intermediate filament. |
| DUSP7 | 0.5 | 0.46 | Dual specific phosphatase 7 |
| PKP3 | 0.49 | 0.52 | Plakophilin 3. Desmosome/nuclei. |
| HES2 | 0.48 | 0.55 | Hes family bHLH transcription factor 2 |
| RHOV | 0.48 | 0.51 | Ras homolog family member V |
| FRMD8 | 0.48 | 0.47 | FERM domain containing 8 |
| BICD2 | 0.48 | 0.37 | BICD cargo adapter 2 |
| SEMA4B | 0.47 | 0.59 | Semaphorin 4B |
| FAM83A | 0.47 | 0.53 | Family with sequence similarity 83 member A |
| KRT16 | 0.47 | 0.52 | Keratin 16. Intermediate filament. |
| CMIP | 0.47 | 0.51 | c-Maf inducing protein |
| TTC22 | 0.47 | 0.49 | Tetratricopeptide repeat domain 22 |
| DSC3 | 0.47 | 0.49 | Desmocollin 3. Calcium-dependent glycoprotein. |
| ZNF750 | 0.47 | 0.48 | Zinc finger protein 750 |
| BARX2 | 0.47 | 0.45 | BARX homeobox 2. Transcription factor. Cell adhesion/actin cytoskeleton. |
| ARHGEF 4 | 0.47 | 0.42 | Rho guanine nucleotide exchange factor 4 |
| TP63 | 0.46 | 0.54 | Tumor protein p63 |
| RIPK4 | 0.46 | 0.52 | Receptor interacting serine/threonine kinase 4 |
| KCTD1 | 0.46 | 0.52 | Potassium channel tetramerization domain containing 1 |
| KRT6A | 0.46 | 0.46 | Keratin 6A. Type II cytokeratin. Intermediate filament. |
| DSP | 0.46 | 0.44 | Desmoplakin. Intermediate filament anchor to desmosome. |

Based on RNA Seq V2 RSEM data from TCGA human bladder cancer samples (n = 408). P values are <0.00001 for each correlation. Genes highlighted in gray are putative transcription factor/regulators. Basal marker genes KRT5 and KRT6A are highlighted in blue.